1-1-2010

Mechanical, microstructure and texture properties of interstitial-free steel and copper subjected to equal channel angular extrusion and cold-rolling

A A. Gazder
University of Wollongong, azdiar@uow.edu.au

S S. Hazra
University of Wollongong, ssh755@uow.edu.au

C F. Gu
Monash University

W Q. Cao
Monash University

C H J Davies
Monash University

See next page for additional authors

Mechanical, microstructure and texture properties of interstitial-free steel and copper subjected to equal channel angular extrusion and cold-rolling

A A Gazder[1], S S Hazra[1], C F Gu[2], W Q Cao[2], C H J Davies[2], E V Pereloma[1]

[1] School of Mechanical, Materials and Mechatronics Engineering, University of Wollongong, New South Wales 2522, Australia
[2] Department of Materials Engineering, Monash University, Victoria 3800, Australia

azdiar@uow.edu.au

Abstract. Interstitial-free steel and OFHC copper were subjected to 8 passes, route B_C room temperature ECAE followed by cold-rolling up to 97.5% thickness reduction. Uniaxial tensile tests and Electron Back-Scattering Diffraction were used to characterise the evolution in mechanical properties, microstructure refinement and micro-texture. IF-steel showed continuous increase in strength whereas Cu returned reduced strength and a small gain in ductility at 97.5% reduction. In both metals substructure refinement was accompanied by an increase in high-angle boundary fraction, average misorientation and a slight increase in Σ3 boundaries. An evolution of crystallographic orientations from negative shear to predominantly cold-rolled textures after 95% and 97.5% reduction was observed in both metals.

1. Introduction

In order to make commercial use of ultrafine grained materials their behaviour during subsequent deformation into plate/sheet/foil form via cold-rolling (CR) needs to be understood. To-date, adiabatic shear banding in commercial purity Fe was investigated after 4 passes, route C room temperature (RT) Equal Channel Angular Extrusion (ECAE) followed by cryo-rolling up to 82% [1]. The effect of initial grain size on shear banding in ECAE + 95% CR was also studied in Cu [2]. Superplasticity of Al-3Mg-Sc alloys was investigated either by up to 8 passes, route B_C RT-ECAE and CR up to 70% thickness reduction [3] or 4 passes, route B_C ECAE at 473K followed by up to 85% CR [4]. Hcp Ti has also been subjected to ECAE at 673K and further CR up to 73% [5]. Irrespective of material, transmission electron microscopy (TEM) revealed grains elongated in the rolling direction and the retention of high misorientation angles.

The present study compares the effects of additional CR up to 97.5 % reduction on Interstitial-Free (IF) steel and Oxygen-Free High Conductivity (OFHC) copper previously subjected to 8 passes RT-ECAE. Mechanical properties were determined by RT uniaxial tensile testing while Electron Back-Scattering Diffraction (EBSD) returned subgrain/grain statistics, misorientation, Σ3 boundaries and micro-texture.

2. Experimental Procedure

Billets of 80×20×20 mm^3 Ti IF-steel and 120×20×20 mm^3 OFHC Cu were annealed and subjected to N=8 RT-ECAE via route B_C with 10 kN backpressure at 5 and 2 mms^{-1}, respectively. Following this

the billets were further CR for up to 95% (IF-steel) and 97.5% (Cu) thickness reduction. As shown in [6], the rolling direction (RD) was maintained parallel to the prior ECAE extrusion direction (ED).

Flat dog-boned samples of 15(gage)×5×1 mm^3 (IF-steel) and 10×2×1 mm^3 (Cu) were cut from the center of the stable sample length along the ED/RD and subjected to uniaxial tension at strain rates of 8×10^{-4} s^{-1} and 6×10^{-4} s^{-1}, respectively.

ND-ED/RD samples cut from the center of the stable sample cross-section were mechanically ground and electropolished. EBSD was conducted on a JEOL 7001F (IF-steel) and LEO-1350 (Cu) field mission gun-scanning scanning electron microscope fitted with a Nordlys-II detector and the Oxford Channel-5 software package. Operating conditions were 15kV, 1.14nA for IF-steel and 20kV, 5nA for Cu at 20mm working distance. Step sizes of 100, 80 and 25 nm were used for IF-steel and 40 nm for Cu. The maps were initially cleaned using VMAP. Post-processing was undertaken by Channel-5 with a 2° misorientation limit imposed on all maps.

3. Results and Discussion

IF-steel returns greater strength and reducing total elongation (Figure 1, Table 1) with increasing CR reduction. In contrast Cu shows reduced strength and a slight gain in ductility after 97.5% CR. At these imposed strain levels, we expect enhanced dynamic recovery (relative to IF-steel) due to the higher stacking fault energy of Cu [7]. After 95% and 97.5% CR both IF-steel and Cu show a flattening of their tensile curves and reduced rates of decline during Stage-III work hardening. However in contrast to IF-steel, Cu returns a larger period of post-necking elongation.

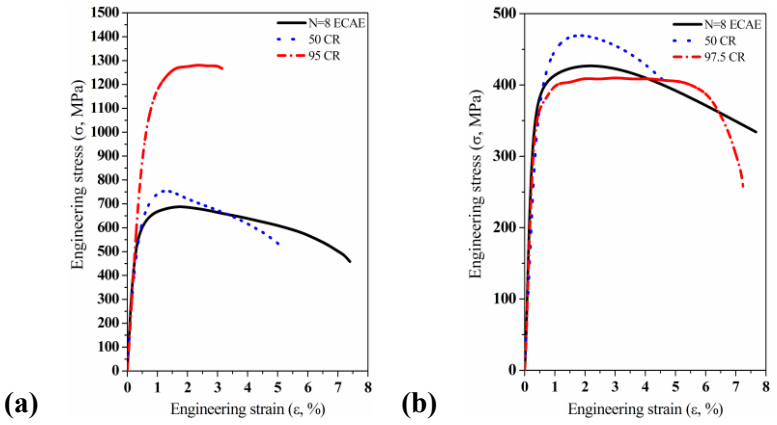

Figure 1. Uniaxial tensile curves of: (a) IF-steel and (b) Cu after N = 8 ECAE and up to 97.5% CR.

Table 1. Mechanical properties of IF steel and Cu after N = 8 ECAE and cold-rolling.

		$\sigma_{0.2}$ (MPa)	σ_{UTS} (MPa)	$\varepsilon_{uniform}$ (%)	ε_{total} (%)
IF-steel	N=8	607 ± 13	689 ± 19	1.8 ± 0.4	7.5 ± 1.8
	50%	639 ± 81	753 ± 58	1.3 ± 0.1	5.1 ± 0.6
	95%	1097 ± 8	1280 ± 3	2.4 ± 0.2	3.2 ± 0.3
Cu	N=8	385 ± 1	427 ± 1	2.2 ± 0.2	7.7 ± 0.2
	50%	419 ± 5	470 ± 4	1.8 ± 0.2	5.0 ± 2
	97.5%	384 ± 2	410 ± 9	3.2 ± 0.2	7.2 ± 2

After N=8 ECAE IF-steel and Cu comprise a mix of equiaxed and elongated substructures (Figures 2(a, d)). Both materials have a large fraction of high-angle boundaries (HABs) (Table 2) with average subgrain (θ≥2°) sizes of 0.43 (IF-steel) and 0.36 (Cu) μm, respectively. Further CR up to 95% and 97.5% produced a convergence of grain (θ≥15°) sizes with subgrain sizes and increase in average misorientation. Importantly, for similar microstructural length-scales 95% CR IF-steel clearly shows shear banding of ribbon-shaped grains whereas 97.5% CR Cu has a mixed morphology of approximately equiaxed grains between layers of elongated substructures and an absence of shear bands (Figure 2(c, f)).

CR produced a rotation of grains such that their long axis coincides with the RD. When the (110) and (111) pole figures of 50% CR IF-steel and Cu are shown in ECAE convention (Figures 3(b, e)) a clockwise rotation around the TD of ~15-20° becomes obvious (compared to Figures 3(a, d)) and corresponds directly to the macroscopic deformation mode.

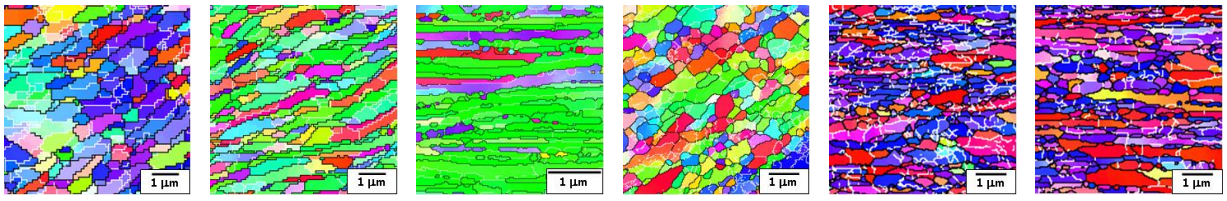

(a) **(b)** **(c)** **(d)** **(e)** **(f)**

Figure 2. Representative inverse pole figure maps of (a-c) IF-steel and (d-f) Cu after: (a, d) N=8 ECAE; (b, e) 50% (c) 95% and (f) 97.5% CR. White lines = LAB ($2°<\theta<15°$); black lines = HAB ($15°\leq\theta\leq62.8°$); green = ⟨101⟩; blue = ⟨111⟩; red = ⟨001⟩; ED/RD = *x-axis*, ND = *y-axis*.

Table 2. Microstructural parameters of IF steel and Cu after N = 8 ECAE and cold-rolling.

		d_{ECD} $\theta\geq2°$ (µm)	d_{ECD} $\theta\geq15°$ (µm)	HAB (%)	Aspect ratio $\theta\geq15°$	θ_{HAB}	θ_{AVG}	Σ3 (%)
IF-steel	N=8	0.43 ± 0.2	0.64 ± 0.4	63 ± 2	2.6 ± 1.3	37.7 ± 0.1	27.3 ± 0.4	2.1 ± 0.5
	50%	0.39 ± 0.2	0.55 ± 0.4	71 ± 2	3.9 ± 2.4	37.9 ± 0.3	29.8 ± 0.8	2.4 ± 0.2
	95%	0.21 ± 0.2	0.25 ± 0.2	85 ± 1	5.1 ± 4.7	39.3 ± 1.6	35.3 ± 1.6	3.4 ± 1.6
Cu	N=8	0.36 ± 0.2	0.56 ± 0.3	57	2.1 ± 0.9	40.1	25.8	1.7
	50%	0.25 ± 0.2	0.39 ± 0.3	63	3.5 ± 2.3	41.1	28.5	3.0
	97.5%	0.28 ± 0.2	0.36 ± 0.3	79	3.6 ± 3.0	41.8	35.0	3.8

After 95% and 97.5% CR both materials clearly depict typical rolling texture components. In IF-steel the highest intensities are noted for $(115)[1\bar{1}0]$ in the α-fiber (⟨110⟩//RD) and $(111)[\bar{1}21]$ in the γ-fiber (⟨111⟩//ND). The former along with {114}⟨110⟩ splits the RD-fiber and is a manifestation of alloying additions [8]. In CR Cu the development of typical Copper-type textures (or the β-fiber) from Copper {112}⟨111⟩ through S {123}⟨634⟩ and ending at Brass {110}⟨112⟩ in φ_2 is seen along with Brass-type textures (or the α-fiber) which includes {011}⟨011⟩, Brass {110}⟨112⟩ and Goss {110}⟨001⟩ in φ_1. After 97.5% CR the maximum volume fraction was found for S (44%) followed by the near Brass orientations (24%), Copper (16%) and Goss (3%).

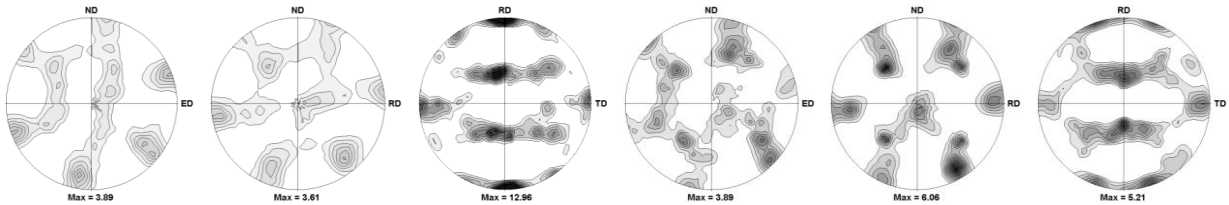

(a) **(b)** **(c)** **(d)** **(e)** **(f)**

Figure 3. (110) and (111) pole figures of of (a-c) IF-steel and (d-f) Cu after: (a, d) N=8 ECAE; (b, e) 50% (c) 95% and (f) 97.5% CR. (a,b) and (d,e) in ECAE convention; (c) and (f) in rolling convention.

The textures in 97.5% CR Cu are mainly Copper-type (α-fiber) but contain an unusually prominent Brass component. Pure Brass textures are ascribed to low stacking fault energy via alloying, reduced rolling temperature and high strain rates. It is associated with late stage shear banding occurring within closely spaced deformation twins via latent hardening [9, 10]. While EBSD mapping resolution is a

limiting factor in this work, the absence of shear banding in ECAE + 97.5% CR Cu agrees with a previous report that attributed its disappearance to the complex deformation path [2].

Of further interest are the small increases in Σ3 boundary fraction in both metals (Table 2). While the twinning domain reduces in bcc materials [11], the opposite occurs in fcc Cu with deformation twins observed in grain interiors and narrow micro-shear bands via TEM [12]. However Σ3 increase in Cu can also be attributed to boundaries being close to S and Brass variants. Again considering the overall scale of deformation twinning, major changes to bulk texture are not expected [10].

Consequently other aspects of 97.5% CR Cu need discussion. Firstly although the Brass intensity is higher than Copper orientation, the former is shared by both β and α -fibers. Since the volume fraction of β-fiber is greater than α-fiber, it corresponds more to a mixed texture state. Secondly, although the rate of grain refinement is markedly faster in IF-steel, the rate of average misorientation increase is quicker in Cu. A greater level of texture symmetry is more readily observed in 50% CR Cu than IF-steel which suggests the texture subdivision of grains.

While Taylor modelling is unsuitable for explaining Brass textures, the composite Sachs model returns approximate agreement only up to 50% CR [10]. Latent hardening simulations assuming quicker hardening rates for previously inactive slip systems have also shown variations in Brass strength at large CR reductions [13]. Thus an alternative approach involving 'slow latent hardening' wherein active slip systems harden at more rapid rates than inactive systems [14] is suggested. Although such assumptions negate shear banding in fcc Cu (an observation that agrees with EBSD) and promotes cross-slip, it could better simulate Brass orientation development for complex deformation paths, large CR reductions and mixed textures.

4. Conclusions

ECAE followed by cold-rolling leads to increases in strength, grain refinement and average misorientation in IF-steel and Cu. Both metals return typical rolling texture components after highest CR reduction. The nature of shear banding in Cu and strength of the Brass component necessitates further investigation into the contributions from deformation twinning and latent hardening.

Acknowledgements

This work was funded under ARC Discovery Project 0557255.

References

[1] Wei Q, Kecskes L, Jiao T, Hartwig K T, Ramesh K T, Ma E, *Acta Mater.* 2004 **52** 1859
[2] Kusnierz J, Baliga W, Bogucka J 2004 Effect of pre-deformation by ECA pressing on shear banding & texture of cold rolled copper *Applied Crystallography: Proc. of XIX Conf.* (Krakow, Poland, 2003) ed H Moraweic, D Stroz (Singapore: World Sci. Pub. Co. Pte. Ltd.) pp. 181
[3] Akamatsu H, Fujinami T, Horita Z, Langdon T G, *Scripta Mater.* 2001 **44** 759
[4] Park K -T, Lee H -J, Lee C S, Shin D H, *Mater. Sci. Eng.* A 2005 **393** 118
[5] Stolyarov V V, Zhu Y T, Alexandrov I V, Lowe T C, Valiev R Z, *Mater. Sci. Eng.* A 2003 **343** 43
[6] Hazra S S, Gazder A A, Pereloma E V, *Mater. Sci. Eng.* A 2009 *doi: 10.1016/j.msea.2009.06.033*
[7] Humphreys F J, Hatherly M 1995 *Recrystallization and Related Annealing Phenomena* (Oxford: Pergamon)
[8] Toroghinejad M R, Ashrafizadeh F, Najafizadeh A, Humphreys A O, Liu D, Jonas J J, *Metall. Mater. Trans.* A 2003 **34**
[9] Leffers T, Pedersen O B, *Scripta Mater.* 2002 **46** 741
[10] Leffers T, Ray R K, *Prog. Mater. Sci.* 2009 **54** 351
[11] Meyers M A, Vöhringer O, Lubarda V A, *Acta Mater.* 2001 **49** 4025
[12] Huang C X, Wang K, Wu S D, Zhang Z F, Li G Y, Li S X, *Acta Mater.* 2006 **54** 655
[13] Miraglia M, Dawson P, Leffers T, *Acta Mater.* 2007 **55** 799
[14] Beyerlein I J, Tomé C N, *Int. J. Plast.* 2007 **23** 640